Title

The Helicobacter pylori CZB Cytoplasmic Chemoreceptor TlpD Forms an Autonomous Polar Chemotaxis Signaling Complex That Mediates a Tactic Response to Oxidative Stress

Journal

Journal of Bacteriology, 198(11)

ISSN

0021-9193

Authors

Collins, Kieran D
Andermann, Tessa M
Draper, Jenny
et al.

Publication Date

2016-06-01

DOI

10.1128/jb.00071-16

Peer reviewed

AMERICAN SOCIETY FOR MICROBIOLOGY | Journal of Bacteriology

The *Helicobacter pylori* CZB Cytoplasmic Chemoreceptor TlpD Forms an Autonomous Polar Chemotaxis Signaling Complex That Mediates a Tactic Response to Oxidative Stress

Kieran D. Collins, Tessa M. Andermann, Jenny Draper, Lisa Sanders, Susan M. Williams, Cameron Araghi, Karen M. Ottemann

Department of Microbiology and Environmental Toxicology, University of California, Santa Cruz, Santa Cruz, California, USA

ABSTRACT

Cytoplasmic chemoreceptors are widespread among prokaryotes but are far less understood than transmembrane chemoreceptors, despite being implicated in many processes. One such cytoplasmic chemoreceptor is *Helicobacter pylori* TlpD, which is required for stomach colonization and drives a chemotaxis response to cellular energy levels. Neither the signals sensed by TlpD nor its molecular mechanisms of action are known. We report here that TlpD functions independently of the other chemoreceptors. When TlpD is the sole chemoreceptor, it is able to localize to the pole and recruits CheW, CheA, and at least two CheV proteins to this location. It loses the normal membrane association that appears to be driven by interactions with other chemoreceptors and with CheW, CheV1, and CheA. These results suggest that TlpD can form an autonomous signaling unit. We further determined that TlpD mediates a repellent chemotaxis response to conditions that promote oxidative stress, including being in the presence of iron, hydrogen peroxide, paraquat, and metronidazole. Last, we found that all tested *H. pylori* strains express TlpD, whereas other chemoreceptors were present to various degrees. Our data suggest a model in which TlpD coordinates a signaling complex that responds to oxidative stress and may allow *H. pylori* to avoid areas of the stomach with high concentrations of reactive oxygen species.

IMPORTANCE

***Helicobacter pylori* senses its environment with proteins called chemoreceptors. Chemoreceptors integrate this sensory information to affect flagellum-based motility in a process called chemotaxis. Chemotaxis is employed during infection and presumably aids *H. pylori* in encountering and colonizing preferred niches. A cytoplasmic chemoreceptor named TlpD is particularly important in this process, and we report here that this chemoreceptor is able to operate independently of other chemoreceptors to organize a chemotaxis signaling complex and mediate a repellent response to oxidative stress conditions. *H. pylori* encounters and must cope with oxidative stress during infection due to oxygen and reactive oxygen species produced by host cells. TlpD's repellent response may allow the bacteria to escape niches experiencing inflammation and elevated reactive oxygen species (ROS) production.**

Chemoreceptors operate on the front line of the bacterial chemotaxis response, sensing signals and initiating attractant or repellent responses. Chemoreceptors can be divided into two classes based on whether they reside in the inner membrane or are soluble cytoplasmic proteins. The cytoplasmic class presumably senses signals that occur intracellularly. Cytoplasmic chemoreceptors are relatively understudied but represent 14% of bacterial and 43% of archaeal chemoreceptors (1). As a group, cytoplasmic chemoreceptors are reported to mediate tactic responses to diverse conditions, including to increased cellular energy stores (2, 3), redox conditions (4, 5), and metabolites (6), although significant gaps remain in our understanding of what they sense and how they function (1). One such cytoplasmic chemoreceptor is *Helicobacter pylori* TlpD. TlpD plays a critical role during *H. pylori* infection of the mammalian stomach (7, 8). In wild-type mice or gerbils, mutant strains of *H. pylori* that lack TlpD display colonization defects during the early stages of infection that are more severe than those of mutant strains that lack any other individual chemoreceptor (7, 8).

TlpD, which was previously referred to as HP0599 or HylB, does not have transmembrane domains and resides in both soluble and membrane-associated subcellular fractions (2). TlpD possesses the canonical chemoreceptor domain, called MA or methyl-accepting chemotaxis receptor protein (MCP) signal, which typically interacts with the signal transduction proteins CheW and CheA. TlpD additionally has a C-terminal zinc-binding domain (CZB) (9, 10), which is the second most prevalent domain found in cytoplasmic chemoreceptors (1). Numerous cytoplasmic chemoreceptors contain a CZB domain and thus share a domain structure with TlpD (1, 9). Chemoreceptors, like TlpD, are widespread and found in many bacterial genera, including gastric and nongastric *Helicobacter* species. CZB domains have been shown to function as zinc-responsive allosteric regulators in diguanylate cyclases (10), but their function in TlpD and other chemoreceptors is not known. Information relating to regulation

Received 20 January 2016 **Accepted** 11 March 2016

Accepted manuscript posted online 21 March 2016

Citation Collins KD, Andermann TM, Draper J, Sanders L, Williams SM, Araghi C, Ottemann KM. 2016. The *Helicobacter pylori* CZB cytoplasmic chemoreceptor TlpD forms an autonomous polar chemotaxis signaling complex that mediates a tactic response to oxidative stress. J Bacteriol 198:1563–1575. doi:10.1128/JB.00071-16.

Editor: I. B. Zhulin

Address correspondence to Karen M. Ottemann, ottemann@ucsc.edu.

of the transcription or translation of *tlpD* is sparse. There is some evidence that *tlpD* and *tlpB* are upregulated in gerbil infections. The regulatory mechanisms, however, are not yet known (11).

The *H. pylori* chemotaxis signal transduction system is reasonably well understood. It contains typical core signaling proteins, the CheA kinase, the CheW coupling protein, and the CheY response regulator, all of which are required for chemotaxis (1, 12, 13). *H. pylori* encodes three transmembrane chemoreceptors called TlpA (HP0099), TlpB (HP0103), and TlpC (HP0082) (7, 8, 12, 14). *H. pylori* also possesses a few accessory chemotaxis signaling proteins that supplement the core ones. In addition to CheW, *H. pylori* expresses three coupling proteins called CheV1, CheV2, and CheV3. CheV proteins combine the CheW coupling domain with an additional phosphorylatable response regulator domain (REC) (15). *H. pylori* CheV proteins all function in chemotaxis, but their exact roles are unclear (17, 19). In *Bacillus subtilis*, CheV modulates CheA activity depending on the covalent modification state of the chemoreceptors and the phosphorylation state of CheV (20). *H. pylori* also encodes two more proteins that are critical for chemotaxis. The first is a CheZ phosphatase, called $CheZ_{HP}$, which is capable of dephosphorylating CheY, CheA, and CheV2 (21). The second is a polyglutamate-rich protein called ChePep. ChePep contains a putative response regulator domain and is conserved in *Epsilonproteobacteria* (22).

Chemotaxis proteins in *H. pylori* are organized into two distinct polar complexes. One complex contains the chemoreceptors CheA and CheV1 (23), while the other contains $CheZ_{HP}$ and ChePep (23). $CheZ_{HP}$ and ChePep physically interact with each other and form a distinct complex at the cell pole that is independent of the one formed by the chemoreceptors and other signaling proteins (23). It is not known why *H. pylori* organizes its chemotaxis proteins into two distinct complexes.

Chemotaxis appears to have the greatest impact on colonization within the first 3 weeks of infection, consistent with the idea that this signal transduction system plays a particularly important role in early *H. pylori* colonization (7, 18, 24–28). *tlpD* mutants are substantially affected in their ability to colonize the stomach at early time points (7, 8), presumably because *tlpD*-deficient strains are unable to sense signals that are generated by exposure to the host environment and are therefore unable to locate a preferred niche in the stomach. At later time points, colonization defects due to chemotaxis and TlpD are less apparent (16, 18). TlpD is reported to mediate a tactic response to electron transport chain inhibitors *in vitro*, a behavior ascribed to energy taxis (2), but it is not yet clear to which signal TlpD responds during such treatment. Studies have shown that *H. pylori* does not display aerotaxis, so a direct oxygen response appears unlikely (16). TlpD has no identifiable domains that would bind reduced flavin adenine dinucleotide ($FADH_2$) or flavin mononucleotide (FMN) at either its N or C terminus, but it has been reported to interact with iron to a small degree (9). Given the important role TlpD plays during host colonization, we sought to understand the function of this chemoreceptor in greater detail. Our results suggest that TlpD is able to operate independently of transmembrane chemoreceptors and coordinates a chemotaxis complex at the pole that contains at least CheA, CheW, CheV1, and CheV3, confirming that it is a bona fide chemoreceptor. Furthermore, we report that TlpD mediates a repellent response to conditions that promote oxidative stress, including being in the presence of iron, hydrogen peroxide, paraquat, and metronidazole. We propose a model in which TlpD-mediated repellent responses to oxidative stress are vital to *H. pylori* avoiding mammalian niches with elevated oxygen, such as near the epithelial surface (29, 30), or reactive oxygen species (ROS) that arise from sites of inflammation (31, 32).

MATERIALS AND METHODS

Bacterial strains and culture conditions. *H. pylori* strains mG27, G27, and SS1 were used for strain construction and experimental studies (Table 1). Other *H. pylori* strains were used to analyze chemoreceptor diversity, as noted in Table 1. *H. pylori* was cultured on either Columbia horse blood agar (CHBA), brucella broth with 10% fetal bovine serum (FBS; Life Technologies) (BB10), or 0.8× Ham's F-12 with 10% FBS (Ham's-10). CHBA consisted of Columbia agar (BD) with 5% defibrinated horse blood (Hemostat Labs, Davis, CA), 50 μg/ml cycloheximide, 10 μg/ml vancomycin, 5 μg/ml cefsulodin, 2.5 U/ml polymyxin B, and 0.2% (wt/vol) β-cyclodextrin. Cultures were incubated at 37°C under 5 to 7% O_2, 10% CO_2, and balance N_2. For the selection of *H. pylori* mutants, 10% (wt/vol) sucrose, 5 to 10 μg/ml chloramphenicol, and 15 μg/ml kanamycin were used. For the selection of plasmid-bearing *Escherichia coli*, 20 μg/ml chloramphenicol, 30 μg/ml kanamycin, and 100 μg/ml ampicillin were used. All media, chemicals, and antibiotics were from BD, Fisher, Sigma, Gold Biosciences, or ISC BioExpress.

Creation of mG27 mutants. Construction of the Δ*cheA*, Δ*tlpA*, Δ*tlpB*, Δ*tlpC*, and Δ*tlpD* mutants has been described (33) (Table 1). Construction of the multiple receptor mutants was described recently (23). In brief, mG27 Δ*tlpA* or Δ*tlpB* was used as the starting strain, and then *tlpC* was eliminated by transformation with plasmid pKO150, or *tlpD* was eliminated by transformation with the Δ*tlpD*::*cat* chromosome from strain KO1006. In all cases, the resulting mutations were verified using PCR.

Motility and chemotaxis analyses. Soft-agar assays were performed using brucella broth, 2.5% (vol/vol) FBS, and 0.35% Bacto agar, as previously described (26). Soft-agar plates were incubated under microaerobic conditions, at 37°C, for 5 to 7 days. To obtain films of swimming *H. pylori*, bacteria were inoculated from plates into 5 ml of Ham's-10 in a 50-ml flask and then incubated with shaking for approximately 15 to 17 h prior to filming. To inspect for tactic responses to extracellular iron or hydrogen peroxide, liquid cultures were checked for motility, diluted to an optical density at 600 nm (OD_{600}) of 0.12 into prewarmed Ham's-10 containing $Fe_2(SO_4)_3$, $FeCl_3$, or H_2O_2 that had been prepared immediately prior to use, at concentrations indicated in the text, and filmed immediately for a maximum duration of 5 min. To inspect for tactic responses to iron chelation or superoxide production, cultures were similarly diluted into 50 μM dipyridyl, 10 μg/ml metronidazole, or 10.5 μM paraquat and then incubated for 15 min under microaerobic conditions. After this period, the cultures were either filmed immediately or treated with $Fe_2(SO_4)_3$, $FeCl_3$, or H_2O_2 and subsequently filmed immediately for a maximum duration of 5 min. The 50% effective concentrations (EC_{50}s) were determined by nonlinear regression of direction change frequencies obtained by tracking wild-type (WT) mG27 exposed to a range of $FeCl_3$ concentrations using GraphPad Prism 6 (GraphPad Software, Inc., San Diego, CA). After mixing, cultures were filmed immediately for a maximum duration of 5 min using phase-contrast microscopy with the SimplePCI software (version 5.2.1.1609; Compix 2003) using a Hamamatsu C4742-95 digital camera mounted on Nikon Eclipse E600 at 400× magnification. Videos were recorded at maximum acquisition speed (approximately 16 frames/s), exported into .AVI format, and then relabeled to blind the analyzer to the condition.

For reversal frequency analysis, individual bacterial swimming paths were analyzed by hand tracing the path of a randomly selected cell that was visible for at least 3 s, with each clear direction change counted, as described previously (34).

Plug bridge spatial chemotaxis assay. For the spatial agarose-in-plug bridge chemotaxis assay, *H. pylori* SS1 was grown to an OD_{600} of 0.2 to 0.8 in BB10 with shaking and then checked for motility. Cells were collected

TABLE 1 Bacterial strains and plasmids used in this study

Strain or plasmid	KO reference no.	Genotype or description	Reference and/or source(s)
Strains			
G27	KO379		69; Nina Salama
mG27	KO625	Mouse-adapted G27	70
mG27 Δ*cheA*	KO629	KO625 Δ*cheA*::*cat*	33
mG27 Δ*tlpA*	KO1002	KO1001 Δ*tlpA*	33
mG27 Δ*tlpB*	KO1004	KO625 Δ*tlpB*	33
mG27 Δ*tlpC*	KO1005	KO625 Δ*tlpC*::*aphA3*	33
mG27 Δ*tlpD*	KO1006	KO625 Δ*tlpD*::*cat*	33
mG27 Δ*tlpA* Δ*tlpC*	KO1008	KO1002 Δ*tlpC*::*aphA3*	23
mG27 Δ*tlpA* Δ*tlpB*	KO1007	KO1022 Δ*tlpB*	23
mG27 Δ*tlpA* Δ*tlpD*	KO1009	KO1002 Δ*tlpD*::*cat*	23
mG27 Δ*tlpB* Δ*tlpD*	KO1012	KO1004 Δ*tlpD*::*cat*	23
mG27 Δ*tlpB* Δ*tlpC*	KO1011	KO1004 Δ*tlpC*::*aphA3*	23
mG27 Δ*tlpC* Δ*tlpD*	KO1013	KO1006 Δ*tlpC*::*aphA3*	23
mG27 Δ*tlpA* Δ*tlpC* Δ*tlpD*	KO1014	KO1009 Δ*tlpC*::*aphA3*	23
mG27 Δ*tlpA* Δ*tlpB* Δ*tlpD*	KO1015	KO1009 Δ*tlpB*	23
mG27 Δ*tlpA* Δ*tlpB* Δ*tlpC*	KO1016	KO1007 Δ*tlpC*::*aphA3*	23
mG27 Δ*tlpB* Δ*tlpC* Δ*tlpD*	KO1017	KO1011 Δ*tlpD*::*cat*	23
mG27 Δ*tlpA* Δ*tlpB* Δ*tlpC* Δ*tlpD*	KO1021	KO1015 Δ*tlpC*::*aphA3*	23
SS1	KO457		71; Janie O'Rourke
SS1 Δ*cheY*	KO481	SS1 Δ*cheY*::*cat-102*	27
SS1 Δ*motB*	KO479	SS1 Δ*motB*::*cat-1*	26
SS1 Δ*tlpA*	KO661	SS1 Δ*tlpA*::*cat*	72
SS1 Δ*tlpB*	KO1108	SS1 Δ*tlpB*::*cat-2*	18
SS1 Δ*tlpC*	KO565	SS1 Δ*tlpC*::*cat*	72
SS1 Δ*tlpD*	KO914	SS1 Δ*tlpD*::*cat-1*	18
SS1 Δ*cheV1*	KO864	SS1 Δ*cheV1*::*cat*	17
SS1 Δ*cheV2*	KO865	SS1 Δ*cheV2*::*cat*	17
SS1 Δ*cheV3*	KO856	SS1 Δ*cheV3*::*cat*	17
SS1 Δ*cheA*	KO855	SS1 Δ*cheA*::*cat*	27
SS1 Δ*cheW*	KO852	SS1 Δ*cheW*::*aphA3*	27
J99	KO479	Wild type	73; Nina Salama
26695	KO668	Wild type	14; ATCC 700392
X47	KO612	Wild type	74; Doug Berg
M6	KO613	Wild type	75; Elizabeth Joyce, Andrew Wright
CPY3401	KO637	Wild type	76; Doug Berg
ATCC 43504	KO669	Wild type	77; ATCC (also known as NCTC 11637)
Alston	KO610	Wild type	78; Elizabeth Joyce
HP 12-1	KO760	Wild type/clinical isolate	Jay Solnick
HP 28-1	KO761	Wild type/clinical isolate	Jay Solnick
HP 116-1	KO764	Wild type/clinical isolate	Jay Solnick
HP 125-1	KO765	Wild type/clinical isolate	Jay Solnick
Plasmid pGEX6P2-CheW		pGEX6p2::CheW	This work

by centrifugation at 2,000 rpm for 5 min at room temperature, washed in phosphate-buffered saline (PBS), resuspended in PBS plus 10% fetal bovine serum (FBS) that had been treated by boiling for 30 min in the presence of 50 mM EDTA, frozen overnight, the liquid portion filtered through a 0.2-μm-pore-size filter, and dialyzed 2 times against a 3,500-kDa dialysis membrane in PBS, as described previously (34). Motility was assessed by microscopy, as described above. The agarose-in-plug bridge assay was carried out as described by Yu and Alam 35), except that the inherent precipitation of $FeCl_3$ was used in place of agarose immobilization. Briefly, two plastic coverslips were placed about 16 mm apart on a glass slide and covered by a glass coverslip. Nine to 100 μl of washed and prepared motile cells was pipetted under the top glass coverslip. Immediately following, 2 μl of 100 mM $FeCl_3$ was pipetted at the edge of the top glass coverslip. The slides were incubated for 15 min under microaerobic conditions, as this duration was empirically determined to lead to a robust chemotactic response. The area immediately surrounding the crystallized iron was observed for the formation of chemotactic bands at 25× magnification using a Zeiss Axiovert 200 inverted microscope, and images were recorded with under bright-field illumination using a Zeiss AxioCam digital camera.

Protein preparation from whole-cell lysates and subcellular fractionation. For whole-cell lysates, total cell proteins were prepared from *H. pylori* cultured on CHBA plates for 2 days. The cells were resuspended in ice-cold PBS. The optical density at 600 nm was determined. The suspension was then mixed with 2× Laemmli sample buffer to give a final OD_{600} of 1.0 and then boiled for 10 min. Five to 10 μl of each sample was separated on a 10% sodium dodecyl sulfate-polyacrylamide gel electrophoresis (SDS-PAGE) gel.

For subcellular fractionation, *H. pylori* strains were grown in 100 ml of BB10 for 24 to 48 h, generating OD_{600}s ranging from 0.24 to 0.55. All

cultures were verified for purity and motility by light microscopy and diluted in BB10 to matching OD_{600}s. *H. pylori* cells were collected by centrifugation at 8,500 × *g* for 10 min at 4°C and resuspended in 1 to 2 ml of lysis buffer [50 mM Tris-HCl (pH 7.0), 10% glycerol, 1 mM 4-(2-aminoethyl) benzenesulfonyl fluoride hydrochloride (AEBSF), 10 mM dithiothreitol (DTT)]. Samples were kept at 4°C on ice for all future steps. Resuspended cells were lysed in bursts by sonication until the lysate appeared clear (3 to 5 min). The lysate was then spun at 349,000 × *g* for 15 min at 4°C in a Beckman TL-100 ultracentrifuge to separate the cytoplasm and membrane fractions. The supernatant (cytoplasm) was removed, and the pellet (membrane fraction) was rinsed three times with 2 ml of high-salt buffer (lysis buffer plus 2 M KCl). The membrane pellet was then completely resuspended in 2 ml of high-salt buffer using an 18-gauge needle and syringe and then collected by centrifugation at 217,000 × *g* for 15 min at 4°C. This step was repeated once more and then repeated again using lysis buffer instead of high-salt buffer. The final membrane pellet was resuspended in a volume of lysis buffer equal to that of the original sample and stored at −20°C. Protein concentration was measured using the Bio-Rad protein assay, with bovine serum albumin (BSA) as a standard. The samples were boiled in Laemmli sample buffer for 5 min and loaded onto 10% SDS-PAGE gels, with an equal total protein concentration in each lane.

Western blotting. Samples run on SDS-PAGE gels were transferred to immunoblot polyvinylidene difluoride (PVDF) membranes (Bio-Rad). Successful transfer and relative protein loading were visualized by staining the membrane with DB71 dye prior to antibody binding. Membranes were incubated with a 1:2,000 to 1:5,000 dilution of anti-glutathione transferase (GST)-TlpA22 (18) or a 1:60 dilution of anti-CheV1 (23). For visualization, the blots were incubated with the horseradish peroxidase-conjugated chicken anti-rabbit or goat anti-rabbit secondary antibody (Santa Cruz Biotechnology) at a dilution of 1:2,000 and incubated with luminol, *p*-coumaric acid, and hydrogen peroxide. Luminescent blots were then exposed to BioMax light film (Kodak) or a Bio-Rad ChemiDoc MP.

Immunofluorescence. Liquid cultures of *H. pylori* wild-type mG27 and *tlpABC* (TlpD only) grown in BB10 to a final OD_{600} of 0.6 to 1.0 were inspected for motility and purity by microscopy prior to fixation on poly-L-lysine-coated slides. Bacteria were fixed and permeabilized as described previously (36) (23). Antibodies were preadsorbed as described previously (23). Preadsorbed anti-His-CheAY (1:200) (23), anti-GST-TlpA22 (1:200) (18), anti-CheV1 (1:100) (23), anti-CheZ (1:200) (23), anti-CheV3 (1:100) (J. Castellon, P. Lertsethtakarn, and K. M. Ottemann, unpublished data), anti-CheW (1:100) (see below), or chicken anti *H. pylori* (AgriSera AB) (1:500) was added, incubated at room temperature for 30 min, and washed with blocking buffer (3% BSA, 0.1% Triton X-100 in 1× PBS) three times. Goat anti-guinea pig antibody–Alexa Fluor 594 or goat anti-chicken antibody–Alexa Fluor 488 (Abcam) was added at a 1:300 or 1:500 dilution, respectively, and incubated in the dark at room temperature for 30 min. The samples were washed with blocking buffer, as described above, and a drop of Vectashield (Vector Laboratories) was added to the samples prior to them being sealed with coverslips. Imaging was performed on a Zeiss LSM 5 Pascal confocal microscope. Images were taken separately in each channel and merged in Adobe Photoshop CS2.

Protein purification and antibody production. *cheW* was amplified from SS1 genomic DNA with the primers cheW623bam (5′-CCCCGGATCCGTGAGCAACCAATTA-3′) and cheW624ecoR1 (5′-CACAGAATTCTTAGAAGTCTTTTTTTAAGATTTC-3′), digested with BamH1 and EcoR1, and ligated into pGEX6P2 (GE Healthcare) to create pGEX6P2-CheW. The resulting plasmid was sequenced to confirm its identity. pGEX6P2-CheW was transformed into ArcticExpress *E. coli* (Agilent), grown to OD_{600} of 0.6, induced with 1 mM isopropyl-β-D-thiogalactopyranoside (IPTG), and expressed at 10°C for 24 h. After overexpression, GST-CheW was purified essentially as described for other GST chemotaxis proteins (21). Protein concentrations were determined using the Bradford assay (Bio-Rad) with BSA as a standard. Anti-CheW antibodies were generated in guinea pigs with purified CheW (Cocolico).

RESULTS

TlpD is a bona fide chemoreceptor able to drive a chemotaxis response. Although certain cytoplasmic chemoreceptors have been reported to respond to specific ligands or conditions, it has remained unclear whether those chemoreceptors can function independently of transmembrane chemoreceptors. To begin our studies on TlpD, we first constructed an *H. pylori* strain that expresses TlpD as its sole chemoreceptor, and for comparison, strains with all other combinations of the chemoreceptors. We confirmed that each chemoreceptor is expressed in the absence of the others by Western blotting using an antibody raised against the conserved MA domain of TlpA (18) (Fig. 1A). As reported before for G27-derived strains (33), mG27 expresses only three of the four chemoreceptors, TlpA, TlpB, and TlpD, and these were expressed at similar levels regardless of which other chemoreceptors were present, although there were some degradation products detected in TlpB-only strains (Fig. 1A). Strains lacking all chemoreceptor genes displayed no antibody cross-reactivity, consistent with the notion that the known chemoreceptors are the only MA domain-containing proteins in mG27 (Fig. 1A). With these strains in hand, we then analyzed whether the sole chemoreceptors were able to confer chemotactic function, using the common brucella broth (BB) plus fetal bovine serum (FBS) soft-agar chemotaxis assay, which has been a valuable method to characterize the chemotaxis system in *H. pylori* (16, 24, 37). Mutant strains that retained only TlpD, referred to as TlpD-only strains, retained near-wild-type chemotaxis, similar to mutants that retained TlpB only (Fig. 1B). These findings are consistent with previous work reporting that TlpD-only mutants retain chemotaxis function in a different assay consisting of conditions that alter cellular energy (2). Strains expressing TlpA only, in contrast, had poor chemotaxis ability (Fig. 1B). Mutants lacking all of the chemoreceptors did not form expanded colonies in this assay, similar to a mutant lacking the key chemotaxis kinase CheA (Fig. 1B), suggesting that there are no other chemotaxis receptors in *H. pylori* that function in this medium. These results suggest that TlpD is able to function on its own to confer chemotaxis.

TlpD has all the information necessary to localize to the pole and assemble a multiprotein chemotaxis signaling complex. The finding that TlpD is able to confer soft-agar migration suggests that it is sufficient to assemble the required chemotaxis signaling proteins. To determine what proteins are assembled by TlpD, we utilized the immunofluorescence of whole cells to visualize the subcellular localization and TlpD dependence of the CheA kinase, the CheW and CheV coupling proteins, and the $CheZ_{HP}$ phosphatase. Previous published work showed that chemoreceptors and chemotaxis signaling proteins are all polar in wild-type *H. pylori* (23). In TlpD-only strains, we observed that TlpD localized to the pole, suggesting that it contains the information needed for this subcellular localization (Fig. 2). CheA, CheW, CheV1, and CheV3 likewise localized to the cell pole in a TlpD-dependent manner (Fig. 2). In contrast, the localization of $CheZ_{HP}$ did not require chemoreceptors, consistent with its localization to an independent complex, as shown previously (23). These results suggest that TlpD has the information necessary to establish and maintain polar localization of itself and to form a

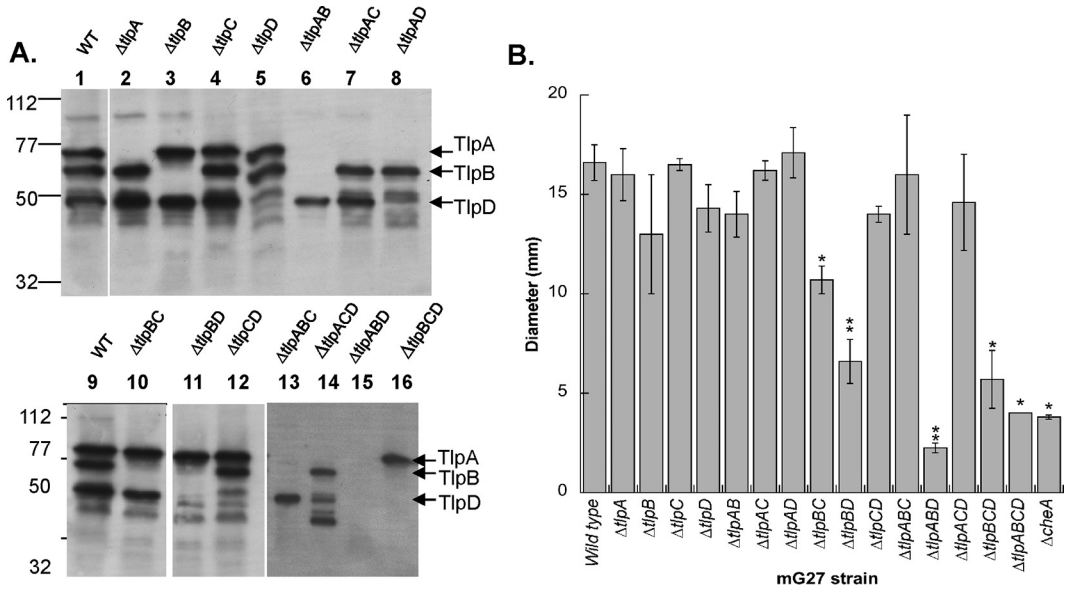

FIG 1 TlpD is stably produced when the sole chemoreceptor confers chemotactic function in a soft-agar assay. (A) Whole-cell lysates were analyzed by Western blotting with the anti-TlpA22 antibody that recognizes all four *H. pylori* chemoreceptors (18). Lane 1, wild-type mG27 (WT); lane 2, mG27 Δ*tlpA*; lane 3, mG27 Δ*tlpB*; lane 4, mG27 Δ*tlpC*; lane 5, mG27 Δ*tlpD*; lane 6, mG27 Δ*tlpA* Δ*tlpB* (Δ*tlpAB*); lane 7, mG27 Δ*tlpA* Δ*tlpC* (Δ*tlpAC*); lane 8, mG27 Δ*tlpA* Δ*tlpD* (Δ*tlpAD*); lane 9, mG27 WT; lane 10, mG27 Δ*tlpB* Δ*tlpC* (Δ*tlpBC*); lane 11, mG27 Δ*tlpB* Δ*tlpD* (Δ*tlpBD*); lane 12, mG27 Δ*tlpC* Δ*tlpD* (Δ*tlpCD*); lane 13, mG27 Δ*tlpA* Δ*tlpB* Δ*tlpC* (Δ*tlpABC*); lane 14, mG27 Δ*tlpA* Δ*tlpC* Δ*tlpD* (Δ*tlpACD*); lane 15, mG27 Δ*tlpA* Δ*tlpB* Δ*tlpD* (Δ*tlpABD*); lane 16, mG27 Δ*tlpB* Δ*tlpC* Δ*tlpD* (Δ*tlpBCD*). Not shown is mG27 Δ*tlpA* Δ*tlpB* Δ*tlpC* Δ*tlpD*, which looks identical to lane 15, as both lack *tlpC*. Marker sizes are given in kilodaltons on the left side. The migration positions of TlpA, TlpB, and TlpD are indicated at the right. Western blots are representative of 2 to 5 replicates for each strain. (B) Brucella broth-FBS soft-agar chemotaxis assays with the colonial diameter of the indicated *H. pylori* strains were measured after 5 days. The error bars represent the standard error of the mean. Each strain was analyzed in two to five biological replicates, with ≥3 technical replicates each time. *, $P < 0.05$; **, $P < 0.01$, compared to the wild type using Student's *t* test.

chemotaxis signaling complex containing at least CheW, CheA, CheV1, and CheV3.

TlpD membrane association depends on transmembrane chemoreceptors CheA, CheW, and CheV1. TlpD has been reported to reside in both the membrane and soluble subcellular fractions (2). It has remained unclear, however, how TlpD associates with the membrane, as it does not have transmembrane domains. Given that TlpD and chemotaxis proteins in general exist in multiprotein complexes (Fig. 2) (38), we examined whether any known chemotaxis proteins were required for TlpD to localize with the membrane fraction. *H. pylori* whole-cell lysate was separated into cytoplasmic and washed membrane fractions and probed using an antichemoreceptor antibody (18). TlpD was found in both soluble and membrane-associated fractions in wild-type cells (Fig. 3A), consistent with previous reports using a distinct *H. pylori* strain (2). Both types of subcellular fractions appeared to be substantially pure based on the lack of transmembrane chemoreceptor proteins in the cytoplasmic fraction and the absence of anti-CheV1 cross-reacting cytoplasmic proteins in the membrane fraction (Fig. 3A). In mutants that lack all transmembrane chemoreceptors, the vast majority of TlpD is cytoplasmic (Fig. 3A), suggesting that membrane chemoreceptors promote TlpD membrane association. Consistent with this possibility, the membrane association of TlpD was substantially reduced in strains lacking the core chemotaxis signaling protein CheA or CheW (Fig. 3B), as well as the CheV1 coupling protein (Fig. 3C). Taken together, these data suggest that the TlpD membrane association is indirect, e.g., that TlpD itself does not interact with the membrane and instead relies on the chemotaxis signaling and chemoreceptor proteins.

TlpD drives a chemotaxis response to conditions generated by iron. The specific parameters sensed by TlpD remain unclear. Prior work had shown that this chemoreceptor responds to conditions generated by blockage of the electron transport chain, but the exact TlpD signal is unknown (2). We thus sought to determine additional conditions that are sensed by TlpD. For this approach, we employed the agarose-in-plug bridge spatial gradient-based chemotaxis assay described by Yu and Alam (35) to test many compounds, including metals, amino acids, and organic acids. We detected a positive response with $FeCl_3$. Specifically, we observed that wild-type *H. pylori* formed a sharp band near the edge of a $FeCl_3$ precipitate, allowing for the bacteria to respond to gradients emerging from the source (Fig. 4). In this assay, there were two features. The first was the sharp bacterial band (indicated by arrows in Fig. 4), which was dependent on chemotactic motility, while the other was a clearing zone, which was independent of chemotactic motility (Fig. 4). We therefore focused on the sharp band as an indicator of chemotaxis. Mutants lacking *tlpD* did not form the sharp bacterial band, whereas other single-receptor mutants lacking *tlpA*, *tlpB*, or *tlpC* formed sharp bands similar to the one seen with wild-type cells. No band formed in response to $MnCl_2$, suggesting that the cells respond to the iron and not the chloride portion of $FeCl_3$. We considered the possibility that *tlpD* mutants are generally defective for chemotaxis but concluded this is not the case because they retain nearly normal soft-agar migration (Fig. 1B) and retain the ability to respond chemotactically to acid (34). We determined that iron is released from the immobilized $FeCl_3$ in this assay, using inductively coupled plasma mass spectrometry analysis of the medium around the $FeCl_3$. We found levels that were 2.5-fold higher than that of background, equiva-

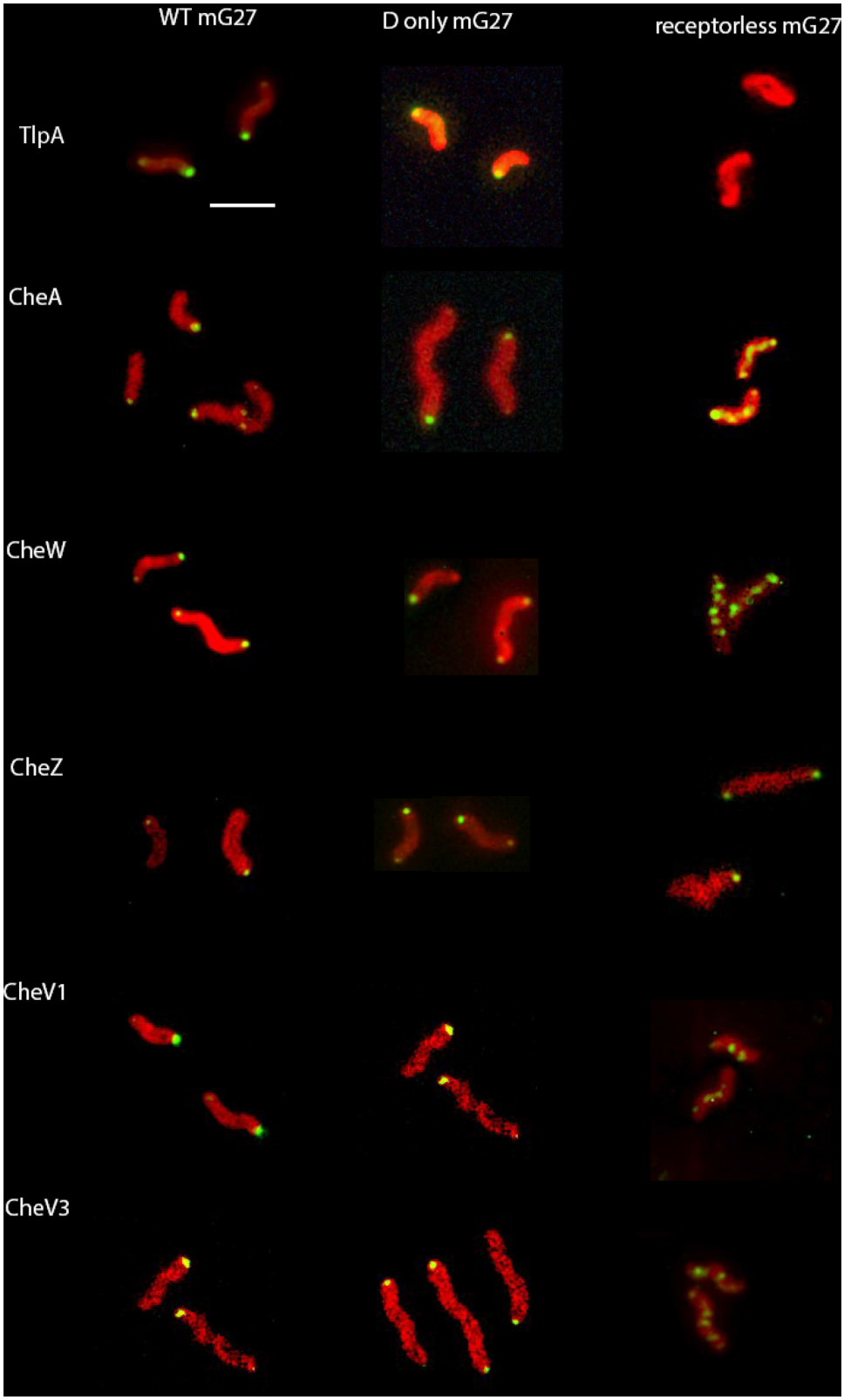

FIG 2 TlpD localizes to the pole and coordinates a chemotaxis complex there. Immunofluorescence images of wild-type (WT), TlpD only (D only), and a strain lacking all chemoreceptors (receptorless, Δ*tlpABCD*) mG27 *H. pylori* strains. *H. pylori* whole cells were detected with chicken anti-*H. pylori* antibodies and stained with goat anti-chicken IgG conjugated to Alexa Fluor 588 (red). Specific chemotaxis proteins were detected as indicated on the left side of the figure, with antibodies as described in Materials and Methods, and subsequently stained with secondary antibodies conjugated to Alexa Fluor 494 (green). The TlpA antibody recognizes all *H. pylori* chemoreceptors. Scale bar = 4 μm.

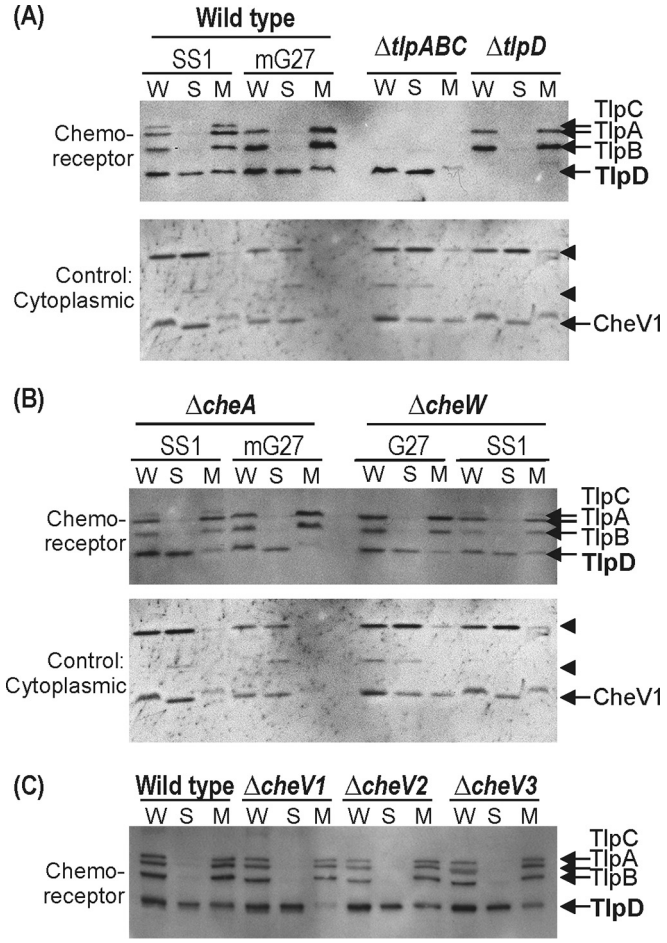

FIG 3 TlpD associates with the membrane fractions via interactions with chemoreceptors and chemotaxis signaling proteins. (A) Top, TlpD subcellular localization in wild-type strains and strains lacking *H. pylori* chemoreceptors, assessed by immunoblotting with anti-TlpA22. W, whole cells; S, soluble; and M, membrane. The positions of the *H. pylori* chemoreceptors TlpA, TlpB, TlpC, and TlpD are shown at the right. Bottom, control blot stripped and reprobed with an anti-CheV1 antibody that additionally recognizes several cytoplasmic proteins (arrowheads). (B) Top, TlpD subcellular localization in strains lacking chemotaxis signaling proteins CheA and CheW, assessed as described in panel A. Bottom, control blot as described in panel A. (C) TlpD subcellular localization in strains lacking chemotaxis signaling proteins CheV1, CheV2, and CheV3, assessed as described in panel A. In all panels, the amount of protein loaded was normalized based on the Bradford assay and confirmed by staining the blots with DB71 (not shown).

lent to 92 nM. We do not know the form of this iron, as the medium contains FBS proteins, so the iron may be chelated by some of these. Additionally, the medium surrounding the iron has a pH of ~5.5 (data not shown), because iron interacts readily with water to form iron hydroxide to liberate protons. The TlpB pH chemoreceptor, however, does not appear to play a role under these conditions. Taken together, these data show that iron is released from $FeCl_3$ in our chemotaxis assay, causes *H. pylori* to form a chemotaxis-dependent band near but not directly adjacent to the immobilized iron, and that TlpD is the only receptor required for this response. These data, however, do not indicate whether the TlpD-dependent chemotactic response to $FeCl_3$ is an attractant or repellent response. The position of the bacterial band a bit away from the iron source, however, suggests that iron may have some repellent properties, as observed previously for other bacteria in their spatial response to oxygen (39).

Iron acts as a TlpD-detected repellent. To determine whether iron was acting as a chemotaxis attractant or repellent, we employed a well-established microscopic assay for *H. pylori* in which the number of bacterial reversals is monitored in response to specific conditions (2, 33, 34). Repellents trigger high numbers of bacterial reversals, while attractants suppress reversals; changes in flagellar rotation have been used in many instances as an accurate indicator of a chemotaxis response (22, 33, 40, 41). This assay has been used to monitor an *H. pylori* repellent response to acid and autoinducer 2 (AI-2); these two conditions cause a 1.5- to 2-fold increase in bacterial reversals (33, 34). Wild-type *H. pylori* showed a statistically significant increase in the frequency of direction changes upon $FeCl_3$ exposure, with an apparent half-maximal effective concentration (EC_{50}) for this response of 100 μM (Fig. 5A). The magnitude of this response, a 1.5-fold increase, is similar to that reported for other *H. pylori* repellents, including acid and AI-2 (33). A concentration of 100 μM of Fe(II) iron sulfate evoked a response similar to that of 100 μM Fe(III)Cl_3 (data not shown). TlpD and chemotaxis signaling were required for this iron-triggered increase in reversals (Fig. 5B). TlpD-only *H. pylori* retained the ability to respond to 100 μM $FeCl_3$ as a repellent, although the change effected by iron was muted compared to that of the wild type and complicated by the fact that this strain already displays a high frequency of reversals (Fig. 5B). Taken together, these results suggest that TlpD mediates a repellent response to iron exposure.

TlpD mediates a repellent response to conditions that promote oxidative stress. While iron is an essential nutrient, it is also toxic because it can react with cellular hydrogen peroxide via Fenton-mediated chemistry to generate reactive oxygen species (ROS), including hydroxyl radical and hydroxide ion (42). Given that iron acted as a repellent, we examined whether ROS might also be a chemotaxis signal for *H. pylori*. We employed the same microscopic swimming assay and assessed the response of *H. pylori* to chemicals shown to generate ROS in *H. pylori*: hydrogen peroxide (43), paraquat (44), and metronidazole (45).

Hydrogen peroxide exposure at 1 mM evoked a repellent response that was TlpD dependent and was retained in a TlpD-only strain (Fig. 5B). A similar response was noted for lower concentrations of hydrogen peroxide at 50 μM, 100 μM, and 500 μM (data not shown). To assess the contribution of Fenton-mediated chemistry in generating conditions sensed by TlpD, *H. pylori* was incubated with the membrane-permeable iron chelator dipyridyl prior to exposure to hydrogen peroxide, using an exposure shown previously to result in intracellular affects within this time frame (46). Dipyridyl pretreatment abolished the TlpD-mediated response to hydrogen peroxide (Fig. 5B). These data suggest that TlpD mediates a chemotaxis response to ROS, and that cytoplasmic iron pools contribute to this response.

To further confirm whether TlpD mediates a response to ROS, we next tested the ability of two superoxide generators, metronidazole and paraquat, to generate TlpD-dependent repellent responses. *H. pylori* strains were incubated in the presence of either metronidazole or paraquat, and swimming behavior was recorded and tracked. Both metronidazole and paraquat exposure induced a TlpD-dependent increase in direction change frequency (Fig. 5C), which was insensitive to the addition or chelation of iron (data not shown). The diluted metronidazole and paraquat did

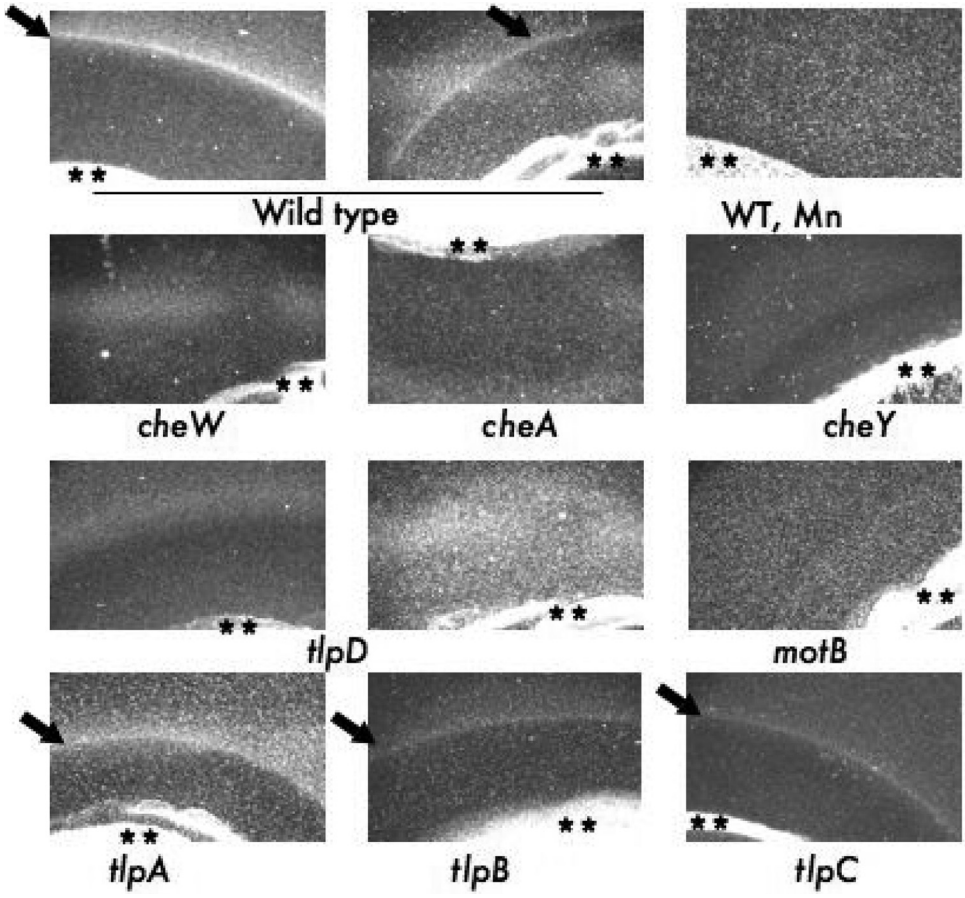

FIG 4 TlpD mediates tactic response to iron in the agarose-in-plug bridge assay. Modified agarose-in-plug bridge assays were carried out using *H. pylori* strain SS1 and its isogenic mutants. The arrows mark chemotactic bacterial rings, and asterisks mark crystallized $FeCl_3$ or $MnCl_2$ in an agarose matrix. Clearing around the plugs is nonspecific, as it appears independently of chemotaxis or motility. Images are representative of the following number of replicates: wild-type, $n = 17$; *cheW*, $n = 1$; *cheA*, $n = 4$; *cheY*, $n = 4$; *tlpA*, $n = 2$; *tlpB*, $n = 4$; *tlpC*, $n = 2$; *tlpD*, $n = 14$; *motB*, $n = 1$.

not affect the pH of the medium with which *H. pylori* was tracked, removing the possibility that the induced repellent responses involved pH sensing. Taken together, these data suggest that TlpD responds to ROS generated by Fenton chemistry as well as superoxide.

TlpD is expressed in all *H. pylori* strains. TlpD is critical for animal infection (7, 8), but previous reports suggested that the expression of TlpD, TlpA, and TlpC varied between *H. pylori* isolates. Specifically, G27 strains express only three chemoreceptors (Fig. 1), and previous studies had suggested that *H. pylori* strains can lack either *tlpC* or *tlpD* (47) or have an interrupted *tlpA* gene (48). It thus was not clear whether TlpD was present, and therefore potentially utilized, by all *H. pylori* strains. We therefore examined the expression of TlpD across different *H. pylori* strains using Western blotting. Of 14 strains examined, all strains expressed TlpD (Fig. 6). All strains also expressed TlpB, but the amount varied substantially (Fig. 6), consistent with a report showing that TlpB expression varies due to a G repeat in the 5′ untranslated region (49). Several strains lacked either TlpC (28%) or TlpA (14%), but no strains lacked both (Fig. 6). The ubiquity of TlpD suggests that it plays critical roles in human infection, in line with its importance in animal models.

DISCUSSION

We report here that the cytoplasmic chemoreceptor TlpD assembles a chemotaxis signaling complex at the pole independently of the transmembrane chemoreceptors, suggesting that TlpD has all the information required for polar localization and signaling complex formation. We furthermore determined that TlpD mediates a repellent response to compounds that generate ROS. Oxygen and ROS are ubiquitous in the stomach, where *H. pylori* resides, arising from both epithelial and immune cells (31, 50). Our findings thus suggest a model in which TlpD is used to help *H. pylori* avoid regions with high ROS, as discussed below.

Previous studies had not addressed whether cytoplasmic chemoreceptors are able to function on their own (1). Here, we show clearly that TlpD is capable of independent function. Specifically, we report that TlpD-only strains can mediate chemotaxis in the soft-agar assay in the absence of transmembrane chemoreceptors, and TlpD-only strains furthermore retain TlpD-mediated chemotaxis responses to ROS. Previous work had shown that TlpD-only strains in a different *H. pylori* background retained the ability to chemotactically respond to electron transport chain inhibition (2), in line with what we report here. We also report that TlpD is sufficient for the formation of polar complexes that con-

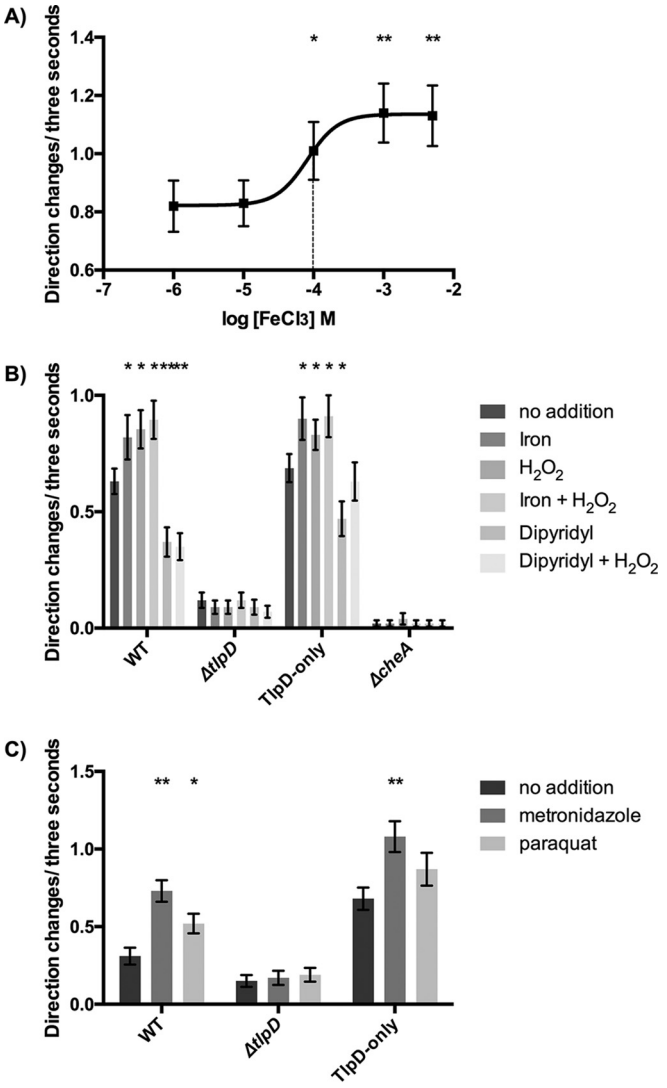

FIG 5 *H. pylori* displays a repellent chemotaxis response to oxidative stress. (A) WT mG27 grown overnight in Ham's-10 was exposed to various concentrations of $FeCl_3$ immediately before being filmed and tracked. Direction changes were tracked over a 3-s window. (B) mG27 strains grown overnight in Ham's-10 were exposed to 100 mM $FeCl_3$, 50 μM dipyridyl, or 1 mM hydrogen peroxide prior to being filmed and tracked. For dipyridyl exposure, cultures were incubated with 50 μM dipyridyl for 15 min prior to addition of $FeCl_3$ or H_2O_2. Direction changes were tracked over a 3 s window. (C) mG27 strains were incubated for 15 min in the presence of either 10 μg/ml metronidazole or 10.5 μM paraquat, swimming behavior was recorded, and direction changes were tracked over a 3-s window. The error bars represent the standard error of the mean. *, $P < 0.05$; **, $P < 0.01$, compared to the wild type using Student's *t* test.

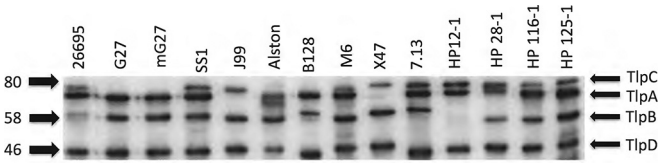

FIG 6 TlpD is expressed by all examined *H. pylori* strains. Chemoreceptor content was analyzed from total cell lysate of the indicated strains using Western blotting with the TlpA22 antibody that recognizes the conserved domain present in all *H. pylori* chemoreceptors (18). Marker sizes are given in kilodaltons on the left. The migration positions of TlpA, TlpB, TlpC, and TlpD are indicated at the right. Western blots are representative of at least 3 replicates for each sample.

tain multiple chemotaxis signaling proteins. Taken together, this work provides strong evidence that TlpD is able to carry out all the necessary functions of a chemoreceptor.

Recent work has visualized cytoplasmic chemoreceptors inside intact cells. Briegel and colleagues (51) identified clusters of cytoplasmic chemoreceptors in *Rhodobacter sphaeroides* and *Vibrio cholerae* that were positioned adjacent to and separate from the transmembrane receptors. These structures showed high similarity in many respects to those produced by transmembrane chemoreceptors, in that the clusters contained trimers of chemoreceptor dimers organized in 12-nm hexagonal arrays (51). These studies, however, were done in wild-type cells that possess multiple chemoreceptors. Our work shows that a soluble chemoreceptor can be sufficient to organize a signaling complex, consistent with the observation that some prokaryotes have only soluble chemoreceptors (1). Polar localization of chemoreceptors is achieved using a variety of mechanisms, including stochastic self-assembly, the use of polar landmark proteins, and ParA orthologues (52). Presumably, TlpD can utilize one or more of these mechanisms, although it is not known which operates in *H. pylori*.

TlpD exists in both soluble and membrane-associated forms, as reported previously (2), and similarly to other cytoplasmic chemoreceptors (1). We found that the association of TlpD with the membrane depends on the transmembrane chemoreceptors CheA, CheW, and CheV1. This finding suggests that TlpD is normally part of the *H. pylori* chemoreceptor signaling complex, interacting with the chemoreceptors via the signaling proteins. Studies in other microbes have also found a role for CheA and CheW in chemoreceptor organization, but the role of the CheV proteins was not well understood. CheV of *B. subtilis* promotes interchemoreceptor clustering of the 10 *B. subtilis* chemoreceptors (53), suggesting that it acts similarly to *H. pylori* CheV1. Of the cytoplasmic chemoreceptors reported to localize to the cell pole, some remain primarily colocalized with transmembrane chemoreceptors (54–56), and others cycle between a diffuse cytoplasmic distribution and a defined polar location (3). It appears that a large fraction of TlpD is soluble in wild-type *H. pylori* strains. It is not clear whether TlpD exists in equilibrium between soluble and membrane-associated states or if membrane association is affected by any signals.

We report here that TlpD mediates a repellent response to conditions that promote oxidative stress, including being in the presence of iron, hydrogen peroxide, paraquat, and metronidazole. Iron was the initial TlpD chemotaxis signal we identified. Chemotactic responses to iron, mediated by TlpD in the agarose-in-plug bridge assay, were confounded by the fact that these tactic responses could be interpreted as repellent, attractant, or mixed attractant and repellent. To clarify the nature of the response, we studied the swimming behavior of *H. pylori* in the presence of iron and noted that the behaviors elicited were consistent with a repellent response. The correlation of swimming behavior and flagellar motor direction changes to chemotactic responses has been used in numerous studies of bacterial chemotaxis across many species (22, 33, 40, 41), and it leant confidence to our conclusion that *H. pylori* was responding to extracellular iron as a repellent. It is possible that iron is a

repellent at high concentration and an attractant at lower concentrations, but we could not detect any such an attractant response even at low concentrations of iron (Fig. 5A).

Because iron acted as a repellent, we focused our attention on its toxic effects, namely, the generation of ROS. Extracellular iron has been documented to rapidly enter the *H. pylori* cytoplasm (57, 58). Specifically, within 5 min of treatment with either iron(III) or iron(II), *H. pylori* had significantly higher levels of intracellular iron than bacteria that did not receive excess iron (57, 58), suggesting that our exposure here would result in intracellular iron increases. Excess iron has been shown carry out Fenton chemistry with endogenous hydrogen peroxide to generate hydroxyl radical and hydroxide anion. Thus, one hypothesis is that iron exposure causes cytoplasmic ROS that are, in turn, the signals sensed by TlpD. Consistent with the idea that elevated cytoplasmic iron propagates ROS, others have found that iron causes a transcriptional response in *H. pylori* genes coding for ROS-detoxifying enzymes (59). In line with this hypothesis, we found that hydrogen peroxide similarly triggered a repellent response, and this response was dependent on free iron (Fig. 5). Iron-ROS connections have additionally been noted in that oxidative stress increases the free cytoplasmic iron pool in *H. pylori* (60). Further support for the idea that TlpD senses ROS came from analysis of other compounds that generate ROS, paraquat and metronidazole, which similarly resulted in a TlpD-mediated repellent response. These data on paraquat and metronidazole suggest that TlpD can respond to superoxide and the hydroxyl radical generated by Fenton chemistry. Although these stresses may be linked (61), TlpD appears to respond independently to the two oxidative stresses in our analyses, because iron chelation did not affect the response to superoxide. Therefore, our results support a model in which TlpD detects several forms of cytoplasmic oxidative stress and leads to a repellent chemotaxis response.

Previous work showed that TlpD additionally mediates a repellent response to electron transport chain inhibitors (2). Interestingly, electron transport chain inhibition is known to generate both hydrogen peroxide and superoxide (61, 62), so it is possible that electron transport inhibitors and ROS affect chemotaxis via the same mechanism. Furthermore, Behrens and colleagues (8) report that *tlpD* mutants are more sensitive than other mutants to oxidative damage, providing an additional connection between TlpD and oxidative stress.

While we know that TlpD is necessary for the ROS response, we do not yet know whether it is sufficient. Chemoreceptors are known to sense signals either directly or via interacting proteins. TlpD has a reported protein interaction partner, HP0697, a predicted subunit of acetone carboxylase (63). This or other unidentified proteins may be required for TlpD's ROS response. Alternatively, TlpD may sense ROS directly, or possibly respond to a small molecule whose concentration changes during oxidative stress. Other proteins use redox-active cofactors, such as FADH, FMN, or iron, to sense alterations in the redox state. These cofactors are typically bound by domains, such as the PAS domain, which are located in the N-terminal direction to the MA domain (1). TlpD has no identifiable domains that would bind FADH or FMN at either its N or C terminus, but it has been reported to interact with iron (9). There are no identifiable domains in the TlpD N-terminal region at all (9), but it does possess a CZB domain at its C terminus, which binds zinc via histidine and cysteine residues (9). As some of us have noted previously (9), other ROS-sensing proteins use cysteine as a way to sense redox status, so this mechanism may operate in TlpD (9).

TlpD is critical during colonization in animal models (7, 8), particularly in the first weeks of infection. *H. pylori* is exposed to ROS produced in the stomach by both epithelial and phagocytic cells (31, 50, 64). The ability to survive ROS appears to be critical during *H. pylori* colonization, as antioxidant enzymes are highly expressed by this microbe, and mutants lacking them are attenuated in colonizing animal hosts (43, 65). Others have documented that epithelial cells of the stomach release hydrogen peroxide that exposes the related *Helicobacter felis* to ROS, consistent with the idea that gastric *Helicobacter* spp. are regularly exposed to ROS (50). Additionally, there is a recently appreciated radial oxygen gradient emanating from the tissue to the lumen of the gastrointestinal tract. While not yet measured in the stomach, the intestinal oxygen gradient is extremely steep, ranging from a tissue level of 160 mm Hg (5.25%) to $<$1 mm Hg (30). These and other findings suggest that near-tissue bacteria are exposed to higher oxygen levels than those in the lumen (29, 66). Indeed, our swimming analysis suggests that room oxygen (21%) acts as a modest *H. pylori* repellent, because dipyridyl decreased the basal bacterial reversal frequency (Fig. 5B), which could be explained by prior reports suggesting that *H. pylori* experiences oxidative stress in atmospheric oxygen (60). ROS affect *H. pylori* cytoplasmic iron concentrations (67), suggesting that the oxidative stress experienced by *H. pylori* is sensitive to oxygen levels in which the bacterium resides. *H. pylori* has been measured to localize within 15 μm of the epithelial surface (68), and it may maintain this distance to limit the oxidative stress it experiences from oxygen and/or reactive oxygen species emanating from the epithelial surface.

In summary, we report that the cytoplasmic chemoreceptor TlpD possesses the key features of a bona fide chemoreceptor: the ability to drive a chemotaxis response and to organize a chemotaxis signaling complex at the pole. TlpD mediates a repellent response to cytosolic ROS. Our work thus adds substantially to our understanding of cytoplasmic chemoreceptors by clearly showing that they independently retain properties, such as polar localization and signaling complex organization, and can promote responses to specific signals.

ACKNOWLEDGMENTS

We thank the Ottemann lab members Yu-Ting Chen for assistance in making some of the plasmids used for the multiple receptor deletions and Pam Lertsethtakarn for creating the CheV3 antibody. We thank Jay Solnick for providing some of the *H. pylori* strains analyzed for chemoreceptor content, John Helmann for helpful discussions about ROS-sensing proteins, and Fitnat Yildiz for careful review of the manuscript.

The project described here was supported by grants AI050000 and AI117345-01 (to K.M.O.) from the National Institute of Allergy and Infectious Diseases (NIAID) at the National Institutes of Health and funds from the University of California Santa Cruz Committee on Research.

The contents of this article are solely the responsibility of the authors and do not necessarily represent the official views of the NIH.

FUNDING INFORMATION

This work, including the efforts of Kieran D. Collins and Karen M. Ottemann, was funded by University of California Santa Cruz Committee on Research. This work, including the efforts of Tessa M. Andermann, Jenny Lyn Draper, Lisa Sanders, Susan M. Williams, Cameron Araghi, and Karen M. Ottemann, was funded by HHS | National Institutes of Health (NIH) (AI050000). This work, including the efforts of Kieran D. Collins and Karen M. Ottemann, was funded by HHS | National Institutes of Health (NIH) (AI117345-01).

REFERENCES

1. **Collins KD, Lacal J, Ottemann KM.** 2014. Internal sense of direction: sensing and signaling from cytoplasmic chemoreceptors. Microbiol Mol Biol Rev **78:**672–684. http://dx.doi.org/10.1128/MMBR.00033-14.
2. **Schweinitzer T, Mizote T, Ishikawa N, Dudnik A, Inatsu S, Schreiber S, Suerbaum S, Aizawa S-I, Josenhans C.** 2008. Functional characterization and mutagenesis of the proposed behavioral sensor TlpD of *Helicobacter pylori*. J Bacteriol **190:**3244–3255. http://dx.doi.org/10.1128/JB.01940-07.
3. **Xie Z, Ulrich LE, Zhulin IB, Alexandre G.** 2010. PAS domain containing chemoreceptor couples dynamic changes in metabolism with chemotaxis. Proc Natl Acad Sci U S A **107:**2235–2240. http://dx.doi.org/10.1073/pnas.0910055107.
4. **Hong CS, Shitashiro M, Kuroda A, Ikeda T, Takiguchi N, Ohtake H, Kato J.** 2004. Chemotaxis proteins and transducers for aerotaxis in *Pseudomonas aeruginosa*. FEMS Microbiology Lett **231:**247–252. http://dx.doi.org/10.1016/S0378-1097(04)00009-6.
5. **Hou S, Larsen RW, Boudko D, Riley CW, Karatan E, Zimmer M, Ordal GW, Alam M.** 2000. Myoglobin-like aerotaxis transducers in *Archaea* and *Bacteria*. Nature **403:**540–544. http://dx.doi.org/10.1038/35000570.
6. **Storch KF, Rudolph J, Oesterhelt D.** 1999. Car: a cytoplasmic sensor responsible for arginine chemotaxis in the archaeon *Halobacterium salinarum*. EMBO J **18:**1146–1158. http://dx.doi.org/10.1093/emboj/18.5.1146.
7. **Rolig AS, Shanks J, Carter JE, Ottemann KM.** 2012. *Helicobacter pylori* requires TlpD-Driven chemotaxis to proliferate in the antrum. Infect Immun **80:**3713–3720. http://dx.doi.org/10.1128/IAI.00407-12.
8. **Behrens W, Schweinitzer T, Bal J, Dorsch M, Bleich A, Kops F, Brenneke B, Didelot X, Suerbaum S, Josenhans C.** 2013. Role of energy sensor TlpD of *Helicobacter pylori* in gerbil colonization and genome analyses after adaptation in the gerbil. Infect Immun **81:**3534–3551. http://dx.doi.org/10.1128/IAI.00750-13.
9. **Draper J, Karplus K, Ottemann KM.** 2011. Identification of a chemoreceptor zinc-binding domain common to cytoplasmic bacterial chemoreceptors. J Bacteriol **193:**4338–4345. http://dx.doi.org/10.1128/JB.05140-11.
10. **Zähringer F, Lacanna E, Jenal U, Schirmer T, Boehm A.** 2013. Structure and signaling mechanism of a zinc-sensory diguanylate cyclase. Structure **21:**1149–1157. http://dx.doi.org/10.1016/j.str.2013.04.026.
11. **Scott DR, Marcus EA, Wen Y, Oh J, Sachs G.** 2007. Gene expression *in vivo* shows that *Helicobacter pylori* colonizes an acidic niche on the gastric surface. Proc Natl Acad Sci U S A **104:**7235–7240. http://dx.doi.org/10.1073/pnas.0702300104.
12. **Lertsethtakarn P, Ottemann KM, Hendrixson DR.** 2011. Motility and chemotaxis in *Campylobacter* and *Helicobacter*. Annu Rev Microbiol **65:**389–410. http://dx.doi.org/10.1146/annurev-micro-090110-102908.
13. **Wuichet K, Zhulin IB.** 2010. Origins and diversification of a complex signal transduction system in prokaryotes. Sci Signal **3:**ra50. http://dx.doi.org/10.1126/scisignal.2000724.
14. **Tomb JF, White O, Kerlavage AR, Clayton RA, Sutton GG, Fleischmann RD, Ketchum KA, Klenk HP, Gill S, Dougherty BA, Nelson K, Quackenbush J, Zhou L, Kirkness EF, Peterson S, Loftus B, Richardson D, Dodson R, Khalak HG, Glodek A, McKenney K, Fitzegerald LM, Lee N, Adams MD, Hickey EK, Berg DE, Gocayne JD, Utterback TR, Peterson JD, Kelley JM, Cotton MD, Weidman JM, Fujii C, Bowman C, Watthey L, Wallin E, Hayes WS, Borodovsky M, Karp PD, Smith HO, Fraser CM, Venter JC.** 1997. The complete genome sequence of the gastric pathogen *Helicobacter pylori*. Nature **388:**539–547. http://dx.doi.org/10.1038/41483.
15. **Alexander RP, Lowenthal AC, Harshey RM, Ottemann KM.** 2010. CheV: CheW-like coupling proteins at the core of the chemotaxis signaling network. Trends Microbiol **18:**494–503. http://dx.doi.org/10.1016/j.tim.2010.07.004.
16. **Croxen MA, Sisson G, Melano R, Hoffman PS.** 2006. The *Helicobacter pylori* chemotaxis receptor TlpB (HP0103) is required for pH taxis and for colonization of the gastric mucosa. J Bacteriol **188:**2656–2665. http://dx.doi.org/10.1128/JB.188.7.2656-2665.2006.
17. **Lowenthal AC, Simon C, Fair AS, Mehmood K, Terry K, Anastasia S, Ottemann KM.** 2009. A fixed-time diffusion analysis method determines that the three *cheV* genes of *Helicobacter pylori* differentially affect motility. Microbiology **155:**1181–1191. http://dx.doi.org/10.1099/mic.0.021857-0.
18. **Williams SM, Chen YT, Andermann TM, Carter JE, McGee DJ, Ottemann KM.** 2007. *Helicobacter pylori* chemotaxis modulates inflammation and bacterium-gastric epithelium interactions in infected mice. Infect Immun **75:**3747–3757. http://dx.doi.org/10.1128/IAI.00082-07.
19. **Pittman MS, Goodwin M, Kelly DJ.** 2001. Chemotaxis in the human gastric pathogen *Helicobacter pylori*: different roles for CheW and the three CheV paralogues, and evidence for CheV2 phosphorylation. Microbiology **147:**2493–2504. http://dx.doi.org/10.1099/00221287-147-9-2493.
20. **Walukiewicz HE, Tohidifar P, Ordal GW, Rao CV.** 2014. Interactions among the three adaptation systems of *Bacillus subtilis* chemotaxis as revealed by an *in vitro* receptor-kinase assay. Mol Microbiol **93:**1104–1118.
21. **Lertsethtakarn P, Ottemann KM.** 2010. A remote CheZ orthologue retains phosphatase function. Mol Microbiol **77:**225–235. http://dx.doi.org/10.1111/j.1365-2958.2010.07200.x.
22. **Howitt MR, Lee JY, Lertsethtakarn P, Vogelmann R, Joubert L-M, Ottemann KM, Amieva MR.** 2011. ChePep controls *Helicobacter pylori* infection of the gastric glands and chemotaxis in the *Epsilonproteobacteria*. mBio **2:**e00098-11. http://dx.doi.org/10.1128/mBio.00098-11.
23. **Lertsethtakarn P, Howitt MR, Castellon J, Amieva MR, Ottemann KM.** 2015. *Helicobacter pylori* $CheZ_{HP}$ and ChePep form a novel chemotaxis-regulatory complex distinct from the core chemotaxis signaling proteins and the flagellar motor. Mol Microbiol **97:**1063–1078. http://dx.doi.org/10.1111/mmi.13086.
24. **Foynes S, Dorrell N, Ward SJ, Stabler RA, McColm AA, Rycroft AN, Wren BW.** 2000. *Helicobacter pylori* possesses two CheY response regulators and a histidine kinase sensor, CheA, which are essential for chemotaxis and colonization of the gastric mucosa. Infect Immun **68:**2016–2023. http://dx.doi.org/10.1128/IAI.68.4.2016-2023.2000.
25. **Eaton KA, Suerbaum S, Josenhans C, Krakowka S.** 1996. Colonization of gnotobiotic piglets by *Helicobacter pylori* deficient in two flagellin genes. Infect Immun **64:**2445–2448.
26. **Ottemann KM, Lowenthal AC.** 2002. *Helicobacter pylori* uses motility for initial colonization and to attain robust infection. Infect Immun **70:**1984–1990. http://dx.doi.org/10.1128/IAI.70.4.1984-1990.2002.
27. **Terry K, Williams SM, Connolly L, Ottemann KM.** 2005. Chemotaxis plays multiple roles during *Helicobacter pylori* animal infection. Infect Immun **73:**803–811. http://dx.doi.org/10.1128/IAI.73.2.803-811.2005.
28. **McGee DJ, Langford ML, Watson EL, Carter JE, Chen YT, Ottemann KM.** 2005. Colonization and inflammation deficiencies in Mongolian gerbils infected by *Helicobacter pylori* chemotaxis mutants. Infect Immun **73:**1820–1827. http://dx.doi.org/10.1128/IAI.73.3.1820-1827.2005.
29. **Espey MG.** 2013. Role of oxygen gradients in shaping redox relationships between the human intestine and its microbiota. Free Radic Biol Med **55:**130–140.
30. **Albenberg L, Esipova TV, Judge CP, Bittinger K, Chen J, Laughlin A, Grunberg S, Baldassano RN, Lewis JD, Li H, Thom SR, Bushman FD, Vinogradov SA, Wu GD.** 2014. Correlation between intraluminal oxygen gradient and radial partitioning of intestinal microbiota. Gastroenterology **147:**1055–1063.e8. http://dx.doi.org/10.1053/j.gastro.2014.07.020.
31. **Handa O, Naito Y, Yoshikawa T.** 2010. *Helicobacter pylori*: a ROS-inducing bacterial species in the stomach. Inflamm Res **59:**997–1003. http://dx.doi.org/10.1007/s00011-010-0245-x.
32. **Cid TP, Fernández MC, Benito Martínez S, Jones NL.** 2013. Pathogenesis of *Helicobacter pylori* infection. Helicobacter **18:**12–17. http://dx.doi.org/10.1111/hel.12076.
33. **Rader BA, Wreden C, Hicks KG, Sweeney EG, Ottemann KM, Guillemin K.** 2011. *Helicobacter pylori* perceives the quorum-sensing molecule AI-2 as a chemorepellent via the chemoreceptor TlpB. Microbiology **157:**2445–2455. http://dx.doi.org/10.1099/mic.0.049353-0.
34. **Sanders L, Andermann TM, Ottemann KM.** 2012. A supplemented soft agar chemotaxis assay demonstrates the *Helicobacter pylori* chemotactic response to zinc and nickel. Microbiology **159:**46–57.
35. **Yu HS, Alam M.** 1997. An agarose-in-plug bridge method to study che-

motaxis in the archaeon *Halobacterium salinarum*. FEMS Microbiology Lett **156:**265–269. http://dx.doi.org/10.1111/j.1574-6968.1997.tb12738.x.
36. **Pentecost M, Otto G, Theriot JA, Amieva MR.** 2006. *Listeria monocytogenes* invades the epithelial junctions at sites of cell extrusion. PLoS Pathog **2:**e3. http://dx.doi.org/10.1371/journal.ppat.0020003.
37. **Beier D, Spohn G, Rappuoli R, Scarlato V.** 1997. Identification and characterization of an operon of *Helicobacter pylori* that is involved in motility and stress adaptation. J Bacteriol **179:**4676–4683.
38. **Briegel A, Li X, Bilwes AM, Hughes KT, Jensen GJ, Crane BR.** 2012. Bacterial chemoreceptor arrays are hexagonally packed trimers of receptor dimers networked by rings of kinase and coupling proteins. Proc Natl Acad Sci U S A **109:**3766–3771. http://dx.doi.org/10.1073/pnas.1115719109.
39. **Mazzag BC, Zhulin IB, Mogilner A.** 2003. Model of bacterial band formation in aerotaxis. Biophys J **85:**3558–3574. http://dx.doi.org/10.1016/S0006-3495(03)74775-4.
40. **Larsen SH, Reader RW, Kort EN, Tso WW, Adler J.** 1974. Change in direction of flagellar rotation is the basis of the chemotactic response in *Escherichia coli*. Nature **249:**74–77. http://dx.doi.org/10.1038/249074a0.
41. **Kihara M, Macnab RM.** 1981. Cytoplasmic pH mediates pH taxis and weak-acid repellent taxis of bacteria. J Bacteriol **145:**1209–1221.
42. **Faulkner MJ, Helmann JD.** 2011. Peroxide stress elicits adaptive changes in bacterial metal ion homeostasis. Antioxid Redox Signal **15:**175–189.
43. **Harris AG, Wilson JE, Danon SJ, Dixon MF, Donegan K, Hazell SL.** 2003. Catalase (KatA) and KatA-associated protein (KapA) are essential to persistent colonization in the *Helicobacter pylori* SS1 mouse model. Microbiology **149:**665–672. http://dx.doi.org/10.1099/mic.0.26012-0.
44. **Wang G, Maier RJ.** 2004. An NADPH quinone reductase of *Helicobacter pylori* plays an important role in oxidative stress resistance and host colonization. Infect Immun **72:**1391–1396. http://dx.doi.org/10.1128/IAI.72.3.1391-1396.2004.
45. **Olekhnovich IN, Goodwin A, Hoffman PS.** 2009. Characterization of the NAD(P)H oxidase and metronidazole reductase activities of the RdxA nitroreductase of *Helicobacter pylori*. FEBS J 3354–3364.
46. **Merrell DS, Thompson LJ, Kim CC, Mitchell H, Tompkins LS, Lee A, Falkow S.** 2003. Growth phase-dependent response of *Helicobacter pylori* to iron starvation. Infect Immun **71:**6510–6525. http://dx.doi.org/10.1128/IAI.71.11.6510-6525.2003.
47. **Gressmann H, Linz B, Ghai R, Pleissner K-P, Schlapbach R, Yamaoka Y, Kraft C, Suerbaum S, Meyer TF, Achtman M.** 2005. Gain and loss of multiple genes during the evolution of *Helicobacter pylori*. PLoS Genet **1:**e43. http://dx.doi.org/10.1371/journal.pgen.0010043.
48. **Cerda O, Rivas A, Toledo HC.** 2003. *Helicobacter pylori* strain ATCC 700392 encodes a methyl-accepting chemotaxis receptor protein (MCP) for arginine and sodium bicarbonate. FEMS Microbiol Lett **224:**175–181. http://dx.doi.org/10.1016/S0378-1097(03)00423-3.
49. **Pernitzsch SR, Tirier SM, Beier D, Sharma CM.** 2014. A variable homopolymeric G-repeat defines small RNA-mediated posttranscriptional regulation of a chemotaxis receptor in *Helicobacter pylori*. Proc Natl Acad Sci U S A **111:**E501–E510. http://dx.doi.org/10.1073/pnas.1315152111.
50. **Grasberger H, El-Zaatari M, Dang DT, Merchant JL.** 2013. Dual oxidases control release of hydrogen peroxide by the gastric epithelium to prevent *Helicobacter felis* infection and inflammation in mice. Gastroenterology **145:**1045–1054. http://dx.doi.org/10.1053/j.gastro.2013.07.011.
51. **Briegel A, Ladinsky MS, Oikonomou C, Jones CW, Harris MJ, Fowler DJ, Chang Y-W, Thompson LK, Armitage JP, Jensen GJ.** 2014. Structure of bacterial cytoplasmic chemoreceptor arrays and implications for chemotactic signaling. Elife **3:**e02151.
52. **Jones CW, Armitage JP.** 2015. Positioning of bacterial chemoreceptors. Trends Microbiol **23:**247–256.
53. **Lamanna AC, Ordal GW, Kiessling LL.** 2005. Large increases in attractant concentration disrupt the polar localization of bacterial chemoreceptors. Mol Microbiol **57:**774–785. http://dx.doi.org/10.1111/j.1365-2958.2005.04728.x.
54. **Bardy SL, Maddock JR.** 2005. Polar localization of a soluble methyl-accepting protein of *Pseudomonas aeruginosa*. J Bacteriol **187:**7840–7844. http://dx.doi.org/10.1128/JB.187.22.7840-7844.2005.
55. **Meier VM, Scharf BE.** 2009. Cellular localization of predicted transmembrane and soluble chemoreceptors in *Sinorhizobium meliloti*. J Bacteriol **191:**5724–5733. http://dx.doi.org/10.1128/JB.01286-08.
56. **Cannistraro VJ, Glekas GD, Rao CV, Ordal GW.** 2011. Cellular stoichiometry of the chemotaxis proteins in *Bacillus subtilis*. J Bacteriol **193:**3220–3227. http://dx.doi.org/10.1128/JB.01255-10.
57. **Velayudhan J, Hughes NJ, McColm AA, Bagshaw J, Clayton CL, Andrews SC, Kelly DJ.** 2000. Iron acquisition and virulence in *Helicobacter pylori*: a major role for FeoB, a high-affinity ferrous iron transporter. Mol Microbiol **37:**274–286. http://dx.doi.org/10.1046/j.1365-2958.2000.01987.x.
58. **Waidner B, Greiner S, Odenbreit S, Kavermann H, Velayudhan J, Stahler F, Guhl J, Bisse E, van Vliet AHM, Andrews SC, Kusters JG, Kelly DJ, Haas R, Kist M, Bereswill S.** 2002. Essential role of ferritin Pfr in *Helicobacter pylori* iron metabolism and gastric colonization. Infect Immun **70:**3923–3929. http://dx.doi.org/10.1128/IAI.70.7.3923-3929.2002.
59. **Ernst FD, Bereswill S, Waidner B, Stoof J, Mäder U, Kusters JG, Kuipers EJ, Kist M, van Vliet AHM, Homuth G.** 2005. Transcriptional profiling of *Helicobacter pylori* Fur- and iron-regulated gene expression. Microbiology **151:**533–546. http://dx.doi.org/10.1099/mic.0.27404-0.
60. **Wang G, Conover RC, Olczak AA, Alamuri P, Johnson MK, Maier RJ.** 2005. Oxidative stress defense mechanisms to counter iron-promoted DNA damage in *Helicobacter pylori*. Free Radic Res **39:**1183–1191. http://dx.doi.org/10.1080/10715760500194018.
61. **Imlay JA.** 2003. Pathways of oxidative damage. Annu Rev Microbiol **57:**395–418.
62. **Hodnick WF, Duval DL, Pardini RS.** 1994. Inhibition of mitochondrial respiration and cyanide-stimulated generation of reactive oxygen species by selected flavonoids. Biochem Pharmacol **47:**573–580. http://dx.doi.org/10.1016/0006-2952(94)90190-2.
63. **Rain JC, Selig L, De Reuse H, Battaglia V, Reverdy C, Simon S, Lenzen G, Petel F, Wojcik J, Schächter V, Chemama Y, Labigne A, Legrain P.** 2001. The protein-protein interaction map of *Helicobacter pylori*. Nature **409:**211–215. http://dx.doi.org/10.1038/35051615.
64. **Ding SZ, Minohara Y, Fan XJ, Wang J, Reyes VE, Patel J, Dirden-Kramer B, Boldogh I, Ernst PB, Crowe SE.** 2007. *Helicobacter pylori* infection induces oxidative stress and programmed cell death in human gastric epithelial cells. Infect Immun **75:**4030–4039. http://dx.doi.org/10.1128/IAI.00172-07.
65. **Seyler RW, Jr, Olson JW, Maier RJ.** 2001. Superoxide dismutase-deficient mutants of *Helicobacter pylori* are hypersensitive to oxidative stress and defective in host colonization. Infect Immun **69:**4034–4040. http://dx.doi.org/10.1128/IAI.69.6.4034-4040.2001.
66. **Marteyn B, West NP, Browning DF, Cole JA, Shaw JG, Palm F, Mounier J, Prévost M-C, Sansonetti P, Tang CM.** 2010. Modulation of *Shigella* virulence in response to available oxygen *in vivo*. Nature **465:**355–358. http://dx.doi.org/10.1038/nature08970.
67. **Wang G, Hong Y, Johnson MK, Maier RJ.** 2006. Lipid peroxidation as a source of oxidative damage in *Helicobacter pylori*: protective roles of peroxiredoxins. Biochim Biophys Acta **1760:**1596–1603. http://dx.doi.org/10.1016/j.bbagen.2006.05.005.
68. **Schreiber S, Konradt M, Groll C, Scheid P, Hanauer G, Werling H-O, Josenhans C, Suerbaum S.** 2004. The spatial orientation of *Helicobacter pylori* in the gastric mucus. Proc Natl Acad Sci U S A **101:**5024–5029. http://dx.doi.org/10.1073/pnas.0308386101.
69. **Censini S, Lange C, Xiang Z, Crabtree JE, Ghiara P, Borodovsky M, Rappuoli R, Covacci A.** 1996. *cag*, a pathogenicity island of *Helicobacter pylori*, encodes type I-specific and disease-associated virulence factors. Proc Natl Acad Sci U S A **93:**14648–14653. http://dx.doi.org/10.1073/pnas.93.25.14648.
70. **Castillo AR, Arevalo SS, Woodruff AJ, Ottemann KM.** 2007. Experimental analysis of *Helicobacter pylori* transcriptional terminators suggests this microbe uses both intrinsic and factor-dependent termination. Mol Microbiol **67:**155–170. http://dx.doi.org/10.1111/j.1365-2958.2007.06033.x.
71. **Lee A, O'Rourke J, De Ungria MC, Robertson B, Daskalopoulos G, Dixon MF.** 1997. A standardized mouse model of *Helicobacter pylori* infection: introducing the Sydney strain. Gastroenterology **112:**1386–1397. http://dx.doi.org/10.1016/S0016-5085(97)70155-0.
72. **Andermann TM, Chen YT, Ottemann KM.** 2002. Two predicted chemoreceptors of *Helicobacter pylori* promote stomach infection. Infect Immun **70:**5877–5881. http://dx.doi.org/10.1128/IAI.70.10.5877-5881.2002.
73. **Alm RA, Ling L, Moir DT, King BL, Brown ED, Doig PC, Smith DR, Noonan B, Guild BC, deJonge BL, Carmel G, Tummino PJ, Caruso A, Uria-Nickelsen M, Mills DM, Ives C, Gibson R, Merberg D, Mills SD, Jiang Q, Taylor DE, Vovis GF, Trost TJ.** 1999. Genomic-sequence comparison of two unrelated isolates of the human gastric pathogen *Helicobacter pylori*. Nature **397:**176–180. http://dx.doi.org/10.1038/16495.
74. **Akada JK, Ogura K, Dailidiene D, Dailide G, Cheverud JM, Berg DE.** 2003. *Helicobacter pylori* tissue tropism: mouse-colonizing strains can tar-

get different gastric niches. Microbiology **149:**1901–1909. http://dx.doi.org/10.1099/mic.0.26129-0.

75. **Eaton KA, Gilbert JV, Joyce EA, Wanken AE, Thevenot T, Baker P, Plaut A, Wright A.** 2002. *In vivo* complementation of *ureB* restores the ability of *Helicobacter pylori* to colonize. Infect Immun **70:**771–778. http://dx.doi.org/10.1128/IAI.70.2.771-778.2002.
76. **Mizote T, Yoshiyama H, Nakazawa T.** 1997. Urease-independent chemotactic responses of *Helicobacter pylori* to urea, urease inhibitors, and sodium bicarbonate. Infect Immun **65:**1519–1521.
77. **Goodwin CS, Armstrong JA, Chilvers T, Peters M, Collins MD, Sly L, McConnell W, Harper W.** 1989. Transfer of *Campylobacter-Pylori* and *Campylobacter-Mustelae* to *Helicobacter* gen. nov. as *Helicobacter-Pylori* comb. nov. and *Helicobacter Mustelae* comb. nov., respectively. Int J Syst Bacteriol **39:**397–405. http://dx.doi.org/10.1099/00207713-39-4-397.
78. **Joyce EA, Bassler BL, Wright A.** 2000. Evidence for a signaling system in *Helicobacter pylori*: detection of a *luxS*-encoded autoinducer. J Bacteriol **182:**3638–3643. http://dx.doi.org/10.1128/JB.182.13.3638-3643.2000.